第 50 卷第 S1 期
2022 年 12 月

同济大学学报(自然科学版)
JOURNAL OF TONGJI UNIVERSITY(NATURAL SCIENCE)

Vol. 50 No. S1
Dec. 2022

**文章编号:** 0253-374X(2022)S1-0170-06

**DOI:** 10. 11908/j. issn. 0253-374x. 23709

# 带燃料电池增程器的插电式混合动力电动车

Tobias STOLL[1], Hans-Jürgen BERNER[1], Michael BARGENDE[2], André Casal KULZER[2], Holger ENTENMANN[2], Marc REICHENBACHER[2]

(1. 斯图加特汽车工程与车辆发动机研究所(FKFS),斯图加特 70569,德国; 2. 斯图加特大学 汽车工程学院(IFS),斯图加特 70569,德国)

**摘要:** 由于日益严格的立法和公司面临的巨大社会压力,城市配送运输车队的电气化变得越来越重要。本文介绍了一款最大总重为7.5 t的3.5 t改装轻型车。该车有一个串行混合电动动力系统,最大电力牵引功率为150 kW,还有一个60 kW的燃料电池增程器。该车使用一个46 kW•h的电池,平均电压水平为400 V,从而使全电动范围达到120 km。电力驱动由一个感应电机和一个锂锰铁磷酸盐(LMFP)电池以及一个2速变速箱实现。燃料电池系统有一个容量为95 L的燃料箱,压力水平为70 bar,这使得车辆的总里程达400 km。一个质子交换膜(PEM)用于直接使用氢气,其额定功率为1.0 W/cm$^2$。质子交换膜被集成在一个60 kW的燃料电池系统中,用于车辆的车载能源生产。对于空气通道,燃料电池系统有一个电动辅助涡轮增压器,以利用废气的热能。吸入空气的加湿是通过一个水喷射器实现的,该喷射器使用来自排气除湿的水。氢气路径是通过一个喷射器电路和一个用于处理氮气的清洗阀实现的。在下文中,将介绍燃料电池系统的设计和控制。最后,介绍了燃料电池系统运行过程中最重要的影响。

**关键词:** 插电式混合动力; 燃料电池; 城市配送运输

**中图分类号:** U469. 72 **文献标志码:** A

## Plug-In Hybrid Electric Vehicle Concept with Fuel Cell Range Extender for Urban Delivery Transport-Powertrain Concept

*Tobias STOLL[1], Hans-Jürgen BERNER[1], Michael BARGENDE[2], André Casal KULZER[2], Holger ENTENMANN[2], Marc REICHENBACHER[2]*

(1. Research Institute for Automotive Engineering and Powertrain Systems Stuttgart (FKFS), 70569 Stuttgart, Germany; 2. Institute of Automotive Engineering (IFS), University of Stuttgart, 70569 Stuttgart, Germany)

**Abstract:** The electrification of vehicle fleets for urban delivery transport is becoming increasingly important due to ever stricter legislation and the high social pressure on companies. In this paper, a converted 3.5 t light-duty vehicle with a maximum gross weight of 7.5 t is introduced. The vehicle has a serial hybrid electric powertrain with a maximum electric traction power of 150 kW and a 60 kW fuel cell range extender. The vehicle uses a 46 kW·h battery with a 400 V mean voltage level, resulting in a full electric range of 120 km. The electric drive is realized with an induction motor and a lithium-manganese-iron-phosphate (LMFP)-battery as well as a 2-speed gearbox. The fuel cell system has a fuel tank with a 95 L volume and 700 bar pressure level, which enables an overall vehicle range of 400 km. A proton-exchange membrane (PEM), for direct hydrogen application, with a rated power of 1.0 W / cm$^2$ is used. The PEM is integrated in a 60 kW fuel cell system for on-board energy generation on the vehicle. For the air-path the fuel cell system has an electrically assisted turbocharger to use the enthalpy of the exhaust air. The humidification of the intake air is realized with a water injector that uses water from dehumidification of the exhaust air. The hydrogen path is realized with an ejector circuit and a purge-valve for nitrogen disposal. In this paper, the design and control of the fuel cell system is introduced. Finally, the most important effects during the operation of the fuel cell system are presented.

**Key words:** plug-in hybrid; fuel cell; urban delivery transport

## 1 Introduction

Due to further increasing reduction targets for $CO_2$-emission standards in legislation, an increasing share of electrified vehicles needs to be applied on the fleets of car manufactures. Different concepts for

收稿日期: 2022-10-23
第一作者: Tobias STOLL(1990—),男,工学博士,主要研究方向为汽车动力总成模拟。E-mail: tobias stoll@fkfs. de

these electrified vehicles are possible. The range goes from hybrid electric vehicles with no external recharge possibility over hybrid electric vehicles with external recharge possibility up to battery electric vehicles. Each of these vehicle types shows advantages and disadvantages in emissions, cost and technology. In this paper, a closer look on to a plug-in hybrid electric vehicle with fuel cell range extender in is given. The vehicle is a converted 3.5 t light-duty vehicle with a maximum gross weight of 7.5 t and an assumed utilization rate of 0.53[1]. The powertrain uses a full electric powertrain with 150 kW traction power and two energy storages. The first energy storage is a 46 kWh on-board battery, the second a 95 l hydrogen tank with a maximum storage pressure of 700 bar. The vehicle uses a highly efficient fuel cell system. The vehicle and powertrain concept presented here has a high well-to-wheel efficiency due to the technology used. The technology used in the powertrain is extrapolated for the year 2 040[2]. The battery system was specifically optimized for urban delivery traffic and has an acceptable full electric range of 120 km. The fuel tank of the fuel cell range extender can also be designed to be small, as it is only used for longer day trips. The range is sufficient for a delivery tour in urban areas with up to 400 km. The powertrain presented here thus has a low weight, low energy consumption and a resulting high possible payload. In the first part of this paper the powertrain and vehicle configuration are introduced. In the second part a closer look to the developed fuel cell system is given.

## 2 Powertrain and vehicle configuration

For this paper, a converted light commercial vehicle with an extended maximum gross weight of 7.5 t is used. With that modification, the used vehicle is defined as a heavy-duty-vehicle. The used vehicle data for the longitudinal dynamics simulation can be seen in Tab. 1 and is partially retrieved from Ref. [1].

The weight is assumed to be the empty weight of the vehicle, the driver and the resulting weight from a

**Tab.1 Vehicle data for longitudinal dynamics simulation**

| Description | Unit | Value |
|---|---|---|
| Weight | kg | 5390 |
| Frontal area | $m^2$ | 4.27 |
| Drag coefficient | — | 0.30 |
| Rolling resistance coefficient | — | 0.012 |

utilization rate of 0.53. In this case, the utilization rate describes the utilization of the maximum payload of the vehicle. The maximum payload results from the maximum permissible total mass of the vehicle of 7 500 kg minus the vehicle weight and the driver's weight. The resulting maximum payload is 5 085 kg. With a utilization rate of 0.53, the average payload of the vehicle is 2 695 kg and the resulting total mass for the simulation is 5 390 kg. The powertrain configuration of the vehicle[1] can be seen in Fig. 1.

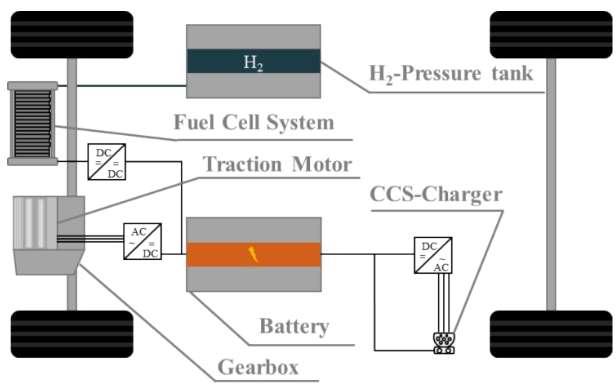


**Fig.1 Powertrain configuration of simulated vehicle[1]**

The powertrain has an electric axle drive on the front-axle with a maximum mechanical output power of 150 kW. The axle drive has an induction motor, with reduced IE-3-efficiency-class, using casted aluminum stator and rotor windings instead of copper [3]. In addition, the electric axle drive uses SiC-MOSFETs for higher switching efficiency of the power electronics module. The efficiency of the electric drive systems, containing the motor and the power electronics module is defined as

$$P_{\mathrm{mech,ED}} = w_{\mathrm{ED}} P_{\mathrm{el,ED}} \tag{1}$$

where $P_{\mathrm{mech,ED}}$ is mechanical power of the electric drive system, $P_{\mathrm{el,ED}}$ is electrical power of the electric drive system, and $w_{\mathrm{ED}}$ is transformation factor of the electric drive system.

The resulting characteristic map, showing the transformation factor for the 150 kW electric drive system is shown in Fig. 2. The bold lines mark the maximum and minimum mechanical torque of the electric drive system.

The transmission of the axle drive contains a 2-speed switchable gearbox as well as a differential gearbox for delivering the traction torque to the road.

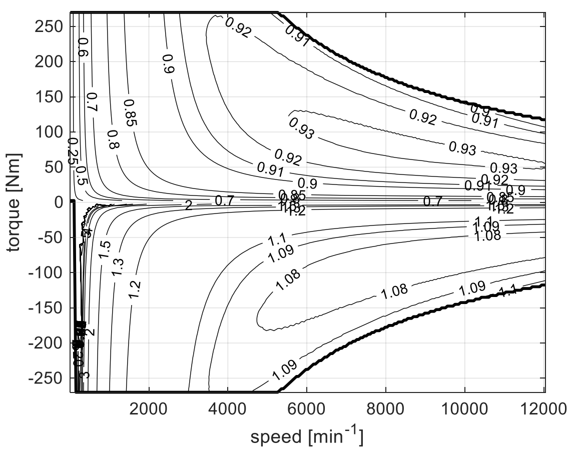


**Fig.2 Characteristic map of motor and power electronics module of electric drive system[1]**

The battery has a mean voltage level of 400 V and a nominal capacity of 46 kW·h. For the anode of the cell carbon nano-graphite particles are used and for the cathode carbon coated lithium-manganese-iron-phosphate. The cells have an estimated gravimetric energy density of 220 W·h/kg and an estimated live time of 1 000 full cycles. The maximum rated charge- and discharge rates are 15 C and −15 C. The usable voltage range of the cells is between 2. 7 V and 4. 35 V to prevent overvoltage and deep discharge of the cells. The fuel cell system has a maximum electrical output power of 60 kW. The fuel is supplied by a 95 L hydrogen tank with a pressure level of 700 bar. The configuration and functionality of the fuel cell system will be introduced in Section 3. The configuration of the powertrain enables a maximum vehicle speed of 130 km/h.

## 3 Fuel cell system

In Fig. 3, the full configuration of the fuel cell system can be seen. The main part of the fuel cell system is the fuel cell stack. The fuel cell stack has an air-supply (light blue) and an exhaust air path (red). These two lines are supplying the cathode of the fuel cell with moisturized and filtered air at a certain pressure level. The fuel supply (green) is fed by the hydrogen tank and provides fuel, at a certain pressure level, for the anode of the fuel cell. The hydrogen is circulated in the anode circuit and delivered by an ejector. The fuel line uses a purge valve to flush diffusing nitrogen out of the fuel circuit to avoid a drop of the cell voltage. The electric part of the fuel cell system (yellow) consists of a DC/DC-converter that delivers electric power to the electrically assisted turbocharger and to the vehicles intermediate circuit. The DC/DC-converter is controlled by the required intermediate circuit voltage of the current operating point. In the following, the functionalities of the fuel cell system are explained and the used components are described. The first functionality is the conversion of hydrogen to electric energy in the fuel cell stack.

For the fuel cell, a predicted cell design for 2040 is used, which is retrieved from Ref. [1]. The cell design shows a low platinum content of 0. 125 mg/cm$^2$, a high general cell voltage of 0. 8 V at 300 m·A/cm$^2$ and a strongly reduced concentration overvoltage, leading to a power density of 1. 0 W/cm$^2$. The membrane live time is assumed to be 8 000 h in automotive applications. The voltage characteristic of the cell design at 80 ℃ stack temperature and 1. 0 bar cathode/anode pressure with fed of air and direct hydrogen can be seen in Fig. 4.

The general configuration of the fuel cell stack can be seen in Tab. 2.

The second functionality is the air supply of the cathode. The air supply is realized with an electrically assisted turbocharger to partially regain the heat in the exhaust air. The electrically assisted turbocharger is chosen to reach maximum efficiency for the air supply of the fuel cell system. Nevertheless, the turbocharger needs to be properly designed due to different particularities for the usage in the fuel cell system:

• Due to lower exhaust air temperatures compared to a combustion engine, the usable

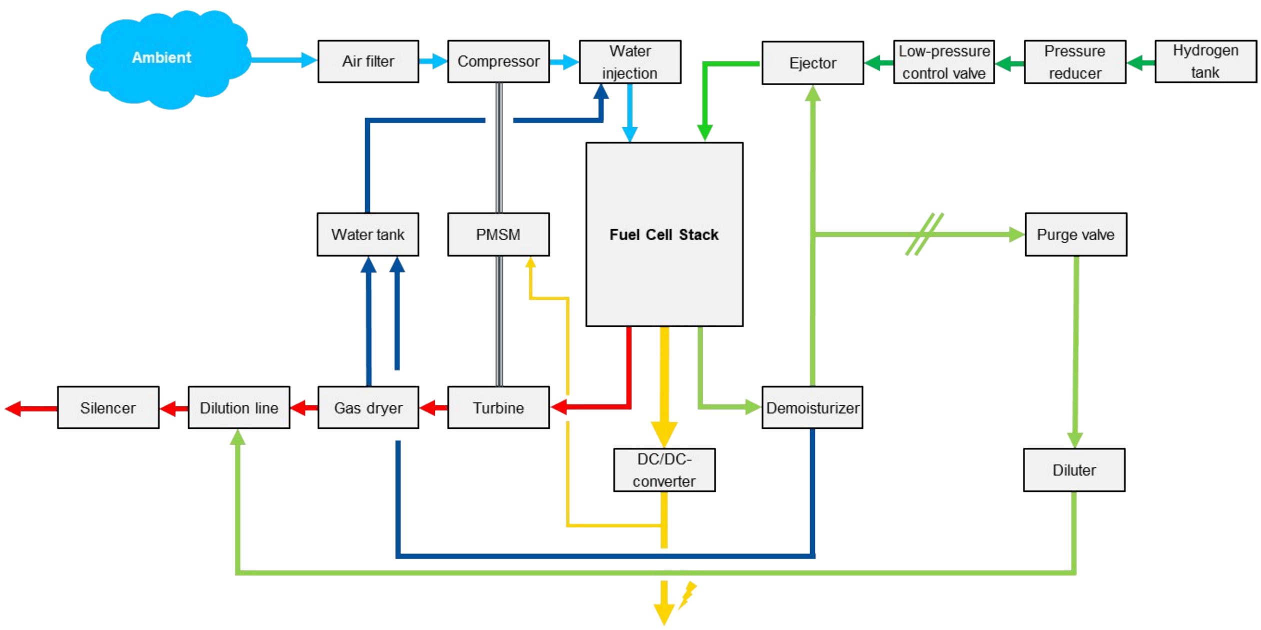


**Fig.3 Overview of components of fuel cell system[2]**

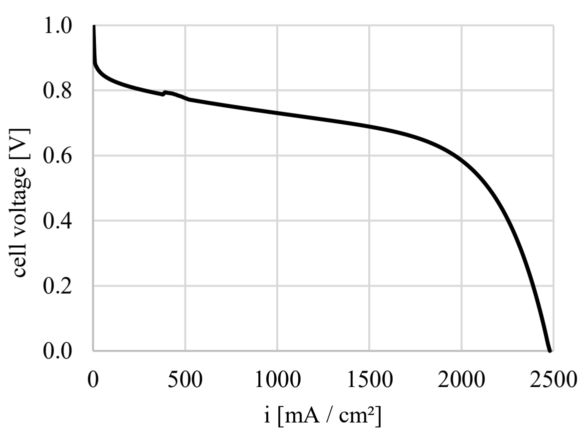


**Fig.4 Voltage characteristic of a predicted 2040 fuel cell design[1]**

**Tab.2 Configuration of fuel cell stack**

| Description | Unit | Value |
|---|---|---|
| Cell area | $mm^2$ | 400 |
| Cell number (serial) | — | 180 |
| Maximum voltage of the Stack | V | 180 |
| Operating temperature | ℃ | 80 |
| Number of gas channels in bipolar plates | — | 5 |
| Number of serpentines in bipolar plates | — | 7 |

enthalpy for the turbine gets lower, which leads to the need of an electrical motor assistance for the compressor.

• The operation pressure of the fuel cell is strongly influenced by the operating points of compressor and turbine and by that by the proper design of the turbocharger.

• The stoichiometry ratio of the intake air is set to $\lambda = 1.1$ to minimize the compressor work or to higher values, if condensation in the turbine occurs in certain operating points.

An optimization with these boundary conditions leads to the turbocharger characteristics shown in Fig. 5, with compressor (left) and turbine (right), with markings for nominal point (60 kW) and maximum efficiency point (15 kW). The optimization for maximum system efficiency leads to a compressor diameter of 45 mm and a turbine wheel diameter of 27.5 mm. The maximum rotational speed of the turbocharger is around 140,000 rad/min. The permanent magnet synchronous motor (PMSM) at the shaft of the turbocharger delivers a maximum torque of 0.35 N·m and has a rated power of 5.5 kW. The air supply also contains an air filter to filter the ambient air and a silencer to reduce the noise induced by the turbocharger. For the water management a water injection is intended which allows easy and fast control of the humidity of the intake air. The water injection works in short pulsed operation to always allow full pressure operation, leading to good stability and mixing of the water jet. The water injector's water supply is provided by the water tank. The water tank level is controlled by the air dryer, which only produces as much water as required to fill the water tank.

The third functionality is the fuel supply of the anode. The anode fuel supply is a closed system, except during purge events. First, the hydrogen delivered by the 700 bar tank system is reduced to 5.0 bar by the pressure reducer. Afterwards, the pressure in the anode circuit is precisely controlled by the low-pressure control valve.

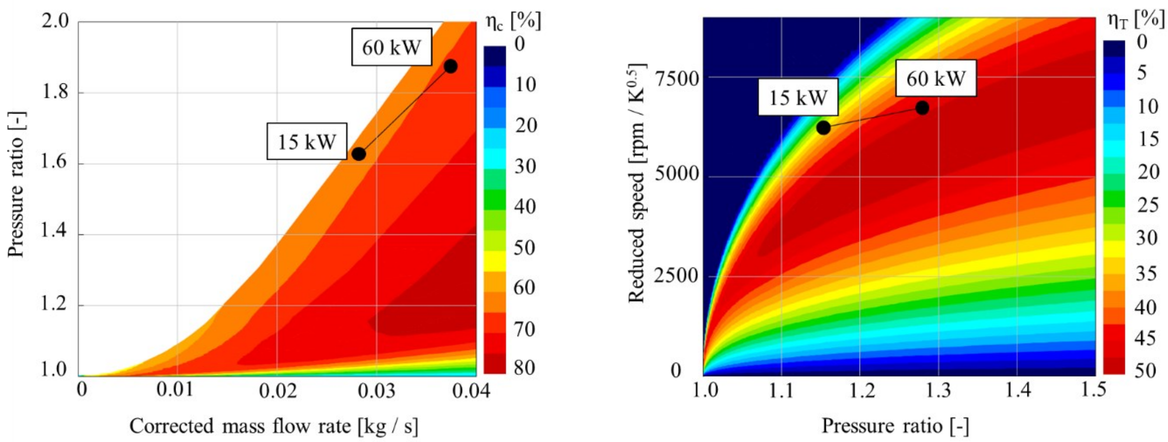


**Fig.5 Efficiency maps of compressor (left) and turbine (right) for maximum efficiency point (15 kW) and nominal point (60 kW)[2]**

Consequently, the mass flow is also controlled with the low-pressure control valve. The ejector or jet pump recirculates the hydrogen in the anode circuit and delivers the needed mass flow to compensate the consumed fuel in the anode circuit. In addition, a passive water demoisturizer is installed to separate the water in the anode circuit, which is transported to the anode side by diffusion through the MEA. The separated water is guided to the water tank, where it is used for humidification of the intake air. The purge valve is used to purge nitrogen out of the anode circuit, if a molar nitrogen concentration of 3% is reached. The purge process lasts until the molar nitrogen concentration is lowered to 1%. During purge events, the pressure in the anode circuit is kept constant by the low-pressure control valve. The purged anode gas is then guided to a passive diluter and from there into the dilution line. The diluter uses a throttle point to continually deliver the purged anode gas to the exhaust air. The diluter is designed to keep the molar hydrogen concentration in the exhaust air below 4%, what corresponds to the lower flammability limit of hydrogen.

The fourth functionality are the electric components of the fuel cell system. The fuel cell systems stack current is controlled by the DC/DC-converter that transforms the electric energy to a requested voltage level for the intermediate circuit of the powertrain. The DC/DC-converter is a buck-boost converter that uses SiC-MOSFETs for control of the output voltage. Due to the more stable voltage conditions, the electrically assisted turbocharger collects its current out of the intermediate circuit of the vehicles powertrain.

The fuel cell systems has a separated system controller and can be seen as a closed system. The external inputs are for example the on/off/standby switch, the power request and the requested voltage level for the electric power output. These parameters are provided by the vehicle's energy management system or the powertrain controller. A schematically display of the control instances for the closed loop control of the fuel cell system can be seen in **Fig. 6**.

The power request controller feeds the feed forward values to the four main controllers of the fuel cell system. The first controller is the cathode pressure control. It controls the electrically assisted turbocharger and manages the airflow to provide the

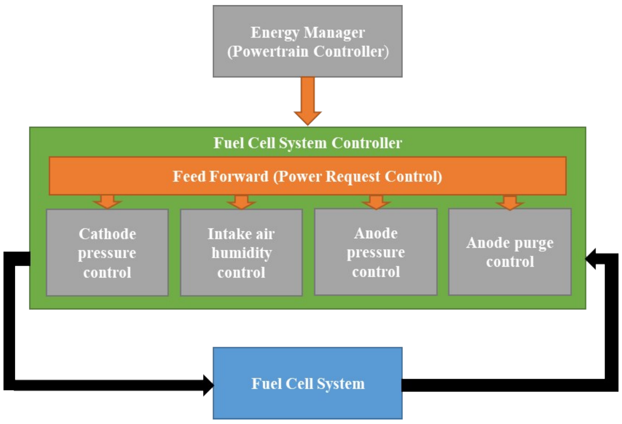


**Fig.6　Closed loop control of fuel cell system[2]**

needed air for the cathode. Additionally, it has safety functions for the turbocharger to avoid compressor stall. For the control, a PI-controller with feed forward is used. The second controller is the intake air humidity control. It controls the water injection, in a manner that the intake air has optimal humidity for humidification of the membrane but avoids condensation in the turbochargers turbine. Also for the intake air humidity control a PI-controller with feed forward is used. The third controller is the anode pressure control. It controls the low-pressure control valve in a manner that the anode pressure always follows the mean cathode pressure. The anode pressure control system works faster than the cathode pressure control. That always assures a pressure equilibrium between anode and cathode. The anode pressure control uses a PI-controller with feed forward. The fourth controller is the anode purge controller. It uses a two-point control that opens at 3% molar fraction of nitrogen in the anode circuit and closes at 1% molar fraction of nitrogen in the anode circuit.

For the resulting overall system efficiency of the fuel cell system, the fuel cell system with controller is put on a virtual test bench. The fuel cell system works at 20 ℃ ambient temperature, 1.0 bar ambient pressure and a mean stack temperature of 80 ℃. Each operating point is than measured for 1 400 s to also include dynamic effects like the purging events. The efficiency is then calculated by setting the lower heating value of the consumed hydrogen in proportion with the electric power output of the system. The electric energy consumption of the electrically assisted turbocharger is also included in the fuel cell system efficiency. The results for the overall system efficiency of the 60 kW fuel cell system can be seen in Fig. 7.

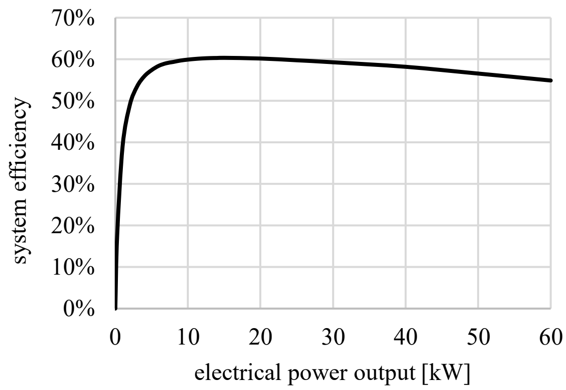


**Fig.7　Overall fuel cell system efficiency referred to the lower heating value of hydrogen[1]**

## 4　Conclusion

In this paper, a fuel cell hybrid electric powertrain with external recharge possibility for a future urban delivery truck is introduced. The powertrain components of the vehicle are described and the installed fuel cell system is discussed in detail. The description contains all four main functions of the fuel cell system (cell stack/air path/fuel path/electric path) as well as the used control approach. The introduced 60 kW fuel cell system reaches a peak efficiency of 60%. Future work will focus on the fuel-optimized operation of the fuel cell system in the presented vehicle as well as on the optimized trajectory planning of the powertrain for suitable driving cycles.

**References:**

[1]　GEB A, LOZANOVSKI A, STOLL T. Potential powertrain configurations to obtain $CO_2$ goals in 2040[R]. Frankfurt am Main: FVV, 2022.

[2]　STOLL T. A simulative approach to predict energy consumption of future powertrain configurations for the year 2040[M]. Wiesbaden: Springer Vieweg, 2023.

[3]　IEC. Rotating electrical machines — Part 30-2: Efficiency classes of variable speed AC motors (IE-code): IEC/TS 60034-30-2[S]. Berlin: Beuth-Verlag, 2019.